J. Phys. Chem. A **1999,** *103,* 7800−7810

Reaction of OH Radical with C_2H_3Cl: Rate Constant and Reaction Pathway Analysis

Li Zhu, Joseph W. Bozzelli,* and Wen-Pin Ho

Department of Chemical Engineering, Chemistry, and Environmental Science, New Jersey Institute of Technology, Newark, New Jersey 07102

Received: February 3, 1999; In Final Form: June 15, 1999

There are two different carbon sites in C_2H_3Cl where OH addition or abstraction reactions can occur, α and β to the Cl atom, with several dissociation and isomerization products of each addition adduct. Thirteen elementary reactions and 18 species are included in the analysis of this reaction system. Thermochemical kinetic parameters are developed for each elementary reaction process. Chemical activation kinetic analysis with multifrequency QRRK theory for $k(E)$ and master equation for falloff are used to estimate overall rate constants as functions of temperature and pressure. Thermodynamic parameters, including $\Delta H_f{}^{\circ}{}_{298}$, $S^{\circ}{}_{298}$, and $C_p{}^{\circ}(T)$ ($300 \leq T/K \leq 1500$), of stable species are from the literature when available or estimated by the group additivity method. Values for $CHClOH\dot{C}H_2$ are determined by density functional calculation and isodesmic reactions. Results are compared with the experimental data. Rate constants (300∼2000 K, in cm^3 mol^{-1} s^{-1}, E_a in cal/mol) for the important addition and abstraction channels at 760 Torr are as follows: $k = 1.22 \times 10^{84}T^{-25.5} \exp(-15000/RT)$ for $C_2H_3Cl + OH \rightarrow CHClOH\dot{C}H_2$; $k = 1.77 \times 10^{40}T^{-9.08} \exp(-7240/RT)$ for $C_2H_3Cl + OH \rightarrow \dot{C}HClCH_2OH$; $k = 9.72 \times 10^{6}T^{2} \exp(-3800/RT)$ for $C_2H_3Cl + OH \rightarrow CH_2{=}\dot{C}Cl + H_2O$; $k = 1.69 \times 10^{7}T^{2} \exp(-4390/RT)$ for $C_2H_3Cl + OH \rightarrow \dot{C}H{=}CHCl + H_2O$.

Introduction

Gas-phase reactions of OH radicals are important in combustion and incineration of chlorinated hydrocarbons as well as in atmospheric chemistry. OH is often the active radical in combustion environments, where it serves to initiate breakdown of hydrocarbons, and it also reacts with CO, producing CO_2 and an H atom plus energy. Here if temperature is high, the H atom may react with O_2 in the critically important chain branching step $H + O_2 \rightarrow OH + O$. Hydroxyl radical is also the most important active species for initiation of atmospheric oxidation processes. It abstracts an H atom from saturated hydrocarbons forming radicals, which then combine with O_2 forming peroxy radicals. The peroxy radicals then react with NO or undergo other reactions related to photochemical smog formation. C−H bonds in olefin, acetylene, and aromatic ring carbons are stronger than the C−H bonds in hydrocarbons, leading to increased barriers for the OH abstraction of H. This results in a change in pathway to that of addition, which has little or no energy barrier. OH addition to unsaturated hydrocarbons and carbonyls form radicals which then further react with O_2 and NO. Previous studies on OH radical reaction with unsaturated hydrocarbons show that the addition reaction predominates at low temperature, while abstraction of an H atom becomes important at high temperature.

Howard[1] has determined the rate constant for reaction of OH with six different ethylene compounds (C_2H_4, C_2H_3Cl, C_2HCl_3, C_2Cl_4, CH_2CF_2, C_2ClF_3) at 296 K and in 0.7−7.0 Torr helium buffer gas, using a discharge-flow reactor with laser magnetic resonance (LMR) detection of OH. The rate constants at 7.0 Torr are all in the range of $(1.2-4.2) \times 10^{12}$ cm^3 mol^{-1} s^{-1}, except for C_2Cl_4 which is lower, about 1.0×10^{11} cm^3 mol^{-1} s^{-1}. The accuracy of the measurements was estimated to be about ±20%. Howard measured eight data points between 0.7 and 7 Torr. These data showed a pressure dependent rate constant for OH reaction with vinyl chloride (in the falloff regime), increasing from 1.2×10^{12} cm^3 mol^{-1} s^{-1} at 0.7 Torr to 3.0×10^{12} cm^3 mol^{-1} s^{-1} at 7.0 Torr.

Perry et al.[2] measured the absolute rate constants for reactions of OH radical with vinyl chloride, vinyl fluoride, and vinyl bromide by using a flash photolysis−resonance fluorescence technique over the temperature range 299−426 K at total pressure of 50 Torr (for C_2H_3Cl and C_2H_3Br) or 100 Torr (for C_2H_3F) in argon. They measured six to eight data points at three temperature (299, 350, and 426 K) for each reaction. The Arrhenius expressions for the rate constants (in cm^3 mol^{-1} s^{-1}) are listed below and show the *k*’s decrease with the increasing temperature:

$$k(C_2H_3F + OH) = 8.91 \times 10^{11}\exp((775 \pm 300)/RT) \text{ or } (3.35 \pm 0.34) \times 10^{12} \text{ at } 298\text{ K};$$

$$k(C_2H_3Cl + OH) = 6.87 \times 10^{11}\exp((1045 \pm 300)/RT) \text{ or } (3.97 \pm 0.40) \times 10^{12} \text{ at } 298\text{ K};$$

$$k(C_2H_3Br + OH) = 1.08 \times 10^{12}\exp((1045 \pm 300)/RT) \text{ or } (4.10 \pm 0.42) \times 10^{12} \text{ at } 298\text{ K}.$$

Comparing these data with the reference high-pressure rate constant for OH + ethylene (4.73×10^{12} cm^3 mol^{-1} s^{-1}), they obtained the following relative rate constants: C_2H_4:C_2H_3Br:C_2H_3Cl:C_2H_3F = 1:0.87:0.84:0.71. This appears to show a trend−the more electronegative the halogen substituent, the lower the rate constant. Perry et al. also reported that variation of total pressure from 52 to 100 Torr for C_2H_3F, and from 50 to 100 Torr for C_2H_3Cl, had no effect on the rate constants within the experimental errors (±5%) at room temperature.

Liu et al.[3] studied the gas-phase reaction of OH radical with

---

* Corresponding author. Phone (973) 596 3459. Fax (973) 642 7179. E-mail: bozzelli@tesla.njit.edu.

10.1021/jp9904015 CCC: $18.00

vinyl chloride at 1 atm of argon over 313−1173 K by using pulse radiolysis, resonant absorption for OH measurement. Temperature dependence of the rate constants showed behavior similar to that of OH + ethylene in that the predominant reaction changed from addition reaction below 588 K to abstraction of hydrogen atom above 723 K. They also observed negative temperature dependence below 588 K and proposed the Arrhenius rate constant (high-pressure limit) for the addition reaction as $1.29 \times 10^{12}\exp((700 \pm 120)/RT)$ cm^3 mol^{-1} s^{-1}. Linear and nonlinear forms of the Arrhenius rate constant for H atom abstraction reaction were reported as $1.79 \times 10^{13}\exp((-4020 \pm 700)/RT)$ and $8.43 \times 10^6 T^2 \exp(-1200/RT)$ cm^3 mol^{-1} s^{-1}, respectively. However, no measurement was made between 588 and 723 K.

Villà et al.[4] used canonical variational transition state theory for the rate constant of OH addition to C_2H_4. Their results show a parabolic form for the addition rate constant versus temperature at PMP4sdtq/6-311+G(d,p)//MP4sdq/6-311+G(d,p)[MP2(FULL)/6-311+G(d,p)] level of calculation. The activation energy is calculated to be −0.92 kcal/mol at 298 K. As temperature increases, the activation energy goes to zero (≈565 K) and then becomes positive. The reactions of OH with C_2H_4, C_2H_3F, and C_2H_3Cl were also recently studied via ab initio calculation at the UMP2/6-311+G(2d,p) level,[5] calculational data including structures of reactants, pre-reaction complexes (van der Waals complexes), transition-states, and radical products. The formation of van der Waals complexes was suggested as a reason for the negative reaction barriers. The enthalpy of the intermediate van der Waals complex was 1.68 kcal/mol lower than the reactants for C_2H_3Cl + OH addition reaction. Results from several calculation levels were compared and showed that the reaction barriers were sensitive to the calculation methods. Kinetic and absolute thermodynamic property data were not reported.

Kleindienst et al.[6] studied production of chlorine atoms from hydroxyl radical addition to chlorinated ethylene using ethylene or propylene as Cl atom scavengers as a means to determine the α to β addition ratio. Mixtures of chloro-unsaturates in 10-fold excess ethylene or propylene/air/NO/C_2H_5ONO were photolyzed, and products of chlorine atom reaction addition with ethylene or propylene were determined.

$$C_2H_3Cl + OH \rightarrow [CHClOH{-}\dot{C}H_2{}^*] \rightarrow CH_2{=}CHOH + Cl$$

$$Cl + C_2H_4 \rightarrow CH_2Cl\dot{C}H_2 \rightarrow (+\,O_2,\ NO) \rightarrow CH_2ClCH_2O^{\bullet} \rightarrow (+O_2) \rightarrow CH_2ClCHO + HO_2$$

Here the stable aldehyde or ketone was monitored. Separate experiments were carried out to calibrate the Cl atom + ethylene and propylene reactions in order to account for the complexities. Kleindienst et al. reported Cl yield from OH reaction with vinyl chloride of 4 ± 1%. This reaction system is complex with complications from the following: short lifetimes resulting in dissociation of the chloroethylene adducts ($k_{\text{dissociation}} \approx 7.5 \times 10^8$ s^{-1}); ClO formation due to Cl + ROO; HO_2 reactions; Cl reaction with NO_2, etc.

C_2H_3Cl + OH addition reactions are complex and nonelementary. OH can add to either α- or β-carbon. In each case, an adduct is formed, which can undergo stabilization via collisions, or before stabilization it may undergo unimolecular reaction to products, or reverse reaction—dissociation back to reactants. There are also two abstraction reactions which can occur: OH can abstract either an α- or a β-H atom.

It would be helpful for both combustion and atmospheric kinetic modeling to know the rate constants and reaction pathways for reaction of OH with vinyl chloride as functions of temperature and pressure. An analysis of OH addition and abstraction reactions to the two carbon atom sites in vinyl chloride is presented in this work. The addition reactions are analyzed by multifrequency QRRK theory for k(E) and master equation analysis as discussed by Gilbert et al.[7] for the falloff. The abstraction reactions are analyzed using the transition-state-theory (TST). Rate constants are calculated using these methods for the addition reactions to specific products versus temperature and pressure.

Methodology

1. Thermodynamic Properties (Table 1). Thermodynamic parameters, $\Delta H_f{}^\circ{}_{298}$, $S^\circ{}_{298}$, $C_p{}^\circ(T)$ ($300 \le T/K \le 1500$), for the reactants, intermediate radicals, and products as well as the corresponding transition state species are listed in Table 1. They are obtained primarily from evaluation of the literature. Thermodynamic properties for some of the oxychlorocarbon species have not been previously measured or calculated; we estimate them using the "THERM" computer code which is based on modified group additivity.[8−13] Bond dissociation energies are from the literature.[14] Hydrogen bond dissociation groups developed by Lay et al.[15] are used to calculate thermodynamic properties of the respective radicals. $S^\circ{}_{298}$ and $C_p{}^\circ(T)$ ($300 \le T/K \le 1500$) of transition states species in the unimolecular reactions are calculated by MOPAC6/PM3,[16,17] where internal rotor contributions to entropies and heat capacities are included by the method of Pitzer and Gwinn.[18−21]

Gas phase thermodynamic parameters for $CHClOHCH_3$ and $CHClOH\dot{C}H_2$ are calculated at B3LYP/6-31G(d,p) level and the isodesmic reactions I−IV, since proper groups for this radical are not available.

$$\underline{CHClOHCH_3} + C_2H_6 \rightarrow C_2H_5OH + C_2H_5Cl \qquad \text{(I)}$$

$$\underline{CHClOHCH_3} + C_2H_5Cl \rightarrow C_2H_5OH + CH_3CHCl_2 \qquad \text{(II)}$$

$$\underline{CHClOH\dot{C}H_2} + C_2H_6 \rightarrow C_2H_5 + CHClOHCH_3 \qquad \text{(III)}$$

$$\underline{CHClOH\dot{C}H_2} + CH_3CHCl_2 \rightarrow \dot{C}H_2CHCl_2 + CHClOHCH_3 \qquad \text{(IV)}$$

Application and advantages of the isodesmic reaction method are described by Lay and Bozzelli[13] and by Yamada et al.[22] Reactions I and II are for $CHClOHCH_3$; reactions III and IV are for $CHClOH\dot{C}H_2$. Energies at 0 K, zero point energies, thermal corrections, and total energies at 298 K for all species in the four isodesmic reactions are listed in Table 2. The established literature enthalpies (in kcal/mol) are −20.20[23] for C_2H_6, −26.80[23] for C_2H_5Cl, −56.17[24] for C_2H_5OH, −31.11[24] for CH_3CHCl_2, 25.89[24] for C_2H_5, and 19.30[24] for $\dot{C}H_2CHCl_2$. From reaction I, we obtain:

$\Delta H_f{}^\circ{}_{298}(CHClOHCH_3) = -56.17 + (-26.80) - (-20.20) - 627.51 \times [(-154.962822) + (-539.362542) - (-79.760847) - (-614.575457)] = -69.64$ kcal/mol

Calculation for reaction II yields $\Delta H_f{}^\circ{}_{298}(CHClOHCH_3) = -70.24$ kcal/mol. So $\Delta H_f{}^\circ{}_{298}$ of $CHClOHCH_3$ is −69.94 kcal/mol from the average of reactions I and II. $\Delta H_f{}^\circ{}_{298}$ of $CHClOH\dot{C}H_2$ is calculated as −21.69 kcal/mol from reactions III and IV. The entropy and heat capacities of $CHClOH\dot{C}H_2$ are calculated based on frequencies and moments of inertia of the optimized B3LYP/6-31G(d,p) structure. Contribution of internal rotors to entropy and heat capacities are calculated separately based on rotational barrier height, foldness, and reduced moments of inertia using the method of Pitzer and

TABLE 1: Thermodynamic Properties[a]

			C_p°											
species	$\Delta H_f^\circ{}_{298}$	$S^\circ{}_{298}$	300 K	400 K	500 K	600 K	800 K	1000 K	1500 K	elements				ref
H	52.10	27.39	4.97	4.97	4.97	4.97	4.97	4.97	4.97		H1			*b*
Cl	29.02	39.45	5.23	5.38	5.44	5.45	5.39	5.32	5.18				Cl1	*c*
HCl	−22.06	44.65	6.96	6.97	7.00	7.07	7.29	7.56	8.14		H1		Cl1	*b*
OH	9.32	43.96	7.15	7.08	7.06	7.06	7.16	7.34	7.89		H1	O1		*c*
CH_2O	−25.98	52.31	8.48	9.39	10.46	11.53	13.38	14.82	17.02	C1	H2	O1		*b*
CH_2Cl	29.10	57.24	10.08	11.45	12.53	13.38	14.66	15.64	17.29	C1	H2		Cl1	*d*
C_2H_3Cl	5.06	63.01	13.00	15.56	17.81	19.70	22.37	24.37	27.44	C2	H3		Cl1	*e*
$CH_2{=}CHOH$	−29.61	62.91	14.15	17.32	19.97	22.08	25.19	27.44	31.09	C2	H4	O1		*e*
$CH_2{=}COHCl$	−39.74	71.71	17.40	19.26	20.83	22.73	25.29	27.28		C2	H3	O1	Cl1	*e*
$CHOH{=}CHCl$	−37.07	70.70	16.95	20.16	22.76	24.78	27.42	29.27	32.15	C2	H3	O1	Cl1	*e*
$\dot{C}H_2CHO$	3.12	60.40	12.92	15.31	17.44	19.24	22.10	24.12		C2	H3	O1		*e*
CH_2ClCHO	−44.41	72.63	15.87	18.61	21.00	23.15	26.35	28.77		C2	H3	O1	Cl1	*e*
$CH_2Cl\dot{C}HOH$	−20.90	77.82	18.36	21.59	24.18	26.30	29.61	32.02		C2	H4	O1	Cl1	*e*
$\dot{C}HClCH_2OH$	−18.30	79.05	18.61	21.60	24.30	26.17	29.48	31.88		C2	H4	O1	Cl1	*e*
$CH_2ClCH_2O^\bullet$	−10.84	75.58	17.05	20.59	23.59	26.08	29.90	32.61		C2	H4	O1	Cl1	*e*
$CHClOH\dot{C}H_2$		70.05	16.05	19.25	21.92	24.09	27.36	29.76	33.66	(TVR)				
		9.09	2.71	2.46	2.31	2.23	2.14	2.09	2.04	(internal rotor)				
	−21.69	79.14	18.76	21.71	24.23	26.32	29.50	31.85	35.70	C2	H4	O1	Cl1	*f*
TS2	(−16.54)	74.44	16.43	19.75	22.52	24.77	28.17	30.68	34.66	C2	H4	O1	Cl1	*g,h*
TS3	(−2.84)	75.93	16.81	19.86	22.49	24.67	28.03	30.54	34.58	C2	H4	O1	Cl1	*g,h*
TS4	(−1.86)	77.21	17.09	20.05	22.62	24.77	28.10	30.59	34.60	C2	H4	O1	Cl1	*g,h*
TS5	(18.48)	75.30	17.90	21.36	24.18	26.41	29.69	32.00	35.53	C2	H4	O1	Cl1	*g,h*
TS6	(7.84)	74.71	15.82	19.16	22.07	24.50	28.27	31.02	35.17	C2	H4	O1	Cl1	*g,h*
TS8	(22.92)	70.34	16.28	20.27	23.63	26.33	30.25	32.93	36.78	C2	H4	O1	Cl1	*g,h*
TS9	(7.93)	74.95	16.51	19.88	22.74	25.06	28.58	31.16	35.16	C2	H4	O1	Cl1	*g,h*
TS10	(7.55)	80.70	20.51	23.98	26.80	29.04	32.35	34.68	38.15	C2	H4	O1	Cl1	*g,h*
TS11	(23.54)	75.06	18.83	22.25	25.00	27.18	30.37	32.60	35.94	C2	H4	O1	Cl1	*g,h*

[a] Radical sites are designated by overhead or superscript bullets; $\Delta H_f^\circ{}_{298}$ in kcal/mol; $S^\circ{}_{298}$ and $C_p^\circ(T)$ in cal/mol·K. TST numbers above correspond to reaction number in Table 3. [b] Reference 23. [c] Reference 41. [d] Enthalpy is from ref 48. Entropy and heat capacities are from MOPAC6/PM3,[16,17] and the comparison with ref 49 shows good agreement. [e] THERM computer code.[9,10] [f] Total TVR internal rotor (see text). TVR is the sum of contributions from translations, external rotations, and vibrations. 18 frequencies based on the optimized B3LYP/6-31G(d,p) structure are 243.2103, 265.2100, 314.4401, 424.8357, 447.7203, 507.8623, 667.9922, 939.0599, 1072.1868, 1163.2286, 1234.8179, 1299.7676, 1436.5185, 1507.6935, 3114.2617, 3188.9373, 3307.0414, and 3810.6613 cm^{-1}. [g] MOPAC6/PM3 plus contributions from internal rotors calculated by Pitzer and Gwinn's method.[18−21] [h] Enthalpies of TS calculated by MOPAC6/PM3 are not used in the rate constant calculations, only shown here as references. For reaction barriers, see Figure 1a,b and Table 3.

TABLE 2: B3LYP/6-31G(d,p) Calculations for Species in Isodesmic Reactions I−IX[a]

species	total energy at 0 K	ZPVE[b]	thermal correction	total energy at 298 K
C_2H_6	−79.838738	0.073470	0.004420	−79.760847
C_2H_5	−79.165207	0.058276	0.004902	−79.102029
C_2H_5Cl	−539.433041	0.065525	0.004974	−539.362542
CH_3CHCl_2	−999.021892	0.056489	0.005783	−998.959620
C_2H_5OH	−155.046670	0.078669	0.005180	−154.962822
$\dot{C}H_2CHCl_2$	−998.344990	0.041131	0.005533	−998.298326
$CHClOHCH_3$	−614.651442	0.070115	0.005870	−614.575457
$CHClOH\dot{C}H_2$	−613.979167	0.055727	0.006167	−613.917273

[a] Units in hartree; 1 hartree = 627.51 kcal/mol. [b] Scaled. Scaling factor is recommended as 0.9806 by Scott and Radom.[50]

Gwinn.[18−21] The thermodynamic parameters for $CHClOH\dot{C}H_2$ are listed in Table 1.

Potential energy diagrams for α- and β-addition are shown in Figures 1a and 1b. Well depths of α- and β-addition are 36.24 and 32.68 kcal/mol at 300 K, and show good agreement with data of Sekušak et al.[5]

2. QRRK Calculations for Analysis of Addition Reactions (Table 3). A modified QRRK (quantum Rice−Ramsperger−Kassel) analysis we use in this paper is described by Chang et al.[25] It is shown to yield reasonable results and provides a framework by which the effects of temperature and pressure can be evaluated in complex reaction systems. The current version of the QRRK computer code utilizes a reduced set of vibration frequencies (usually a set of three frequencies, each degenerate, totaling $3n - 6$), which accurately reproduce the molecule (adduct) heat capacity data. Molecular density of state functions are constructed through direct convolution of single frequency density functions on a 10 cm^{-1} grid. The functions corresponding to each reduced frequency are explicitly convolved into a relative density of states (ρ(E)), which are normalized by the partition function (Q). The inclusion of one external rotation, corresponding to the symmetric top, is incorporated into the calculations by convolving the vibration density function with the proper rotational density function. A detailed description of this and comparisons of ratios of these ρ(E)/Q with direct count ρ(E)/Q are presented in refs 25 and 26. Falloff is incorporated via master equation analysis.[7] $(\Delta E)^\circ_{\text{down}}$ of 1200 cal/mol is used for master equation analysis, N_2 is third body. In this paper we calculate the branching ratios for C_2H_3Cl + OH addition reactions at different temperatures and pressures using the above QRRK chemical activation/falloff analysis. Nonlinear Arrhenius effects resulting from changes in the thermodynamic properties of the respective TST's relative to the adduct with temperature are incorporated using a two-parameter Arrhenius preexponential factor (A, n) in AT^n.

TABLE 3: Input Parameters for the QRRK Calculation of C_2H_3Cl + OH Addition Reactions[a–c]

	reaction	*A*	*n*	E_a	
k_1	$C_2H_3Cl + OH \rightarrow CHClOH\dot{C}H_2$	2.83×10^{11}	0	0	
k_{-1}	$CHClOH\dot{C}H_2 \rightarrow C_2H_3Cl + OH$	1.98×10^{12}	0	34.36	
k_2	$CHClOH\dot{C}H_2 \rightarrow CH_2Cl\dot{C}HOH$	1.88×10^{11}	0.22	6.2	
k_{-2}	$CH_2Cl\dot{C}HOH \rightarrow CHClOH\dot{C}H_2$	9.13×10^{10}	0.22	5.36	α
k_3	$CH_2Cl\dot{C}HOH \rightarrow CH_2{=}CHOH + Cl$	5.23×10^{10}	0.42	19.03	
k_4	$CHClOH\dot{C}H_2 \rightarrow CH_2{=}CHOH + Cl$	9.36×10^{11}	0.19	19.88	
k_5	$CHClOH\dot{C}H_2 \rightarrow CH_2{=}COHCl + H$	2.32×10^{9}	1.06	36.37	
k_6	$CHClOH\dot{C}H_2 \rightarrow \dot{C}H_2CHO + HCl$	1.75×10^{11}	0.23	22	
k_7	$C_2H_3Cl + OH \rightarrow \dot{C}HClCH_2OH$	7.19×10^{11}	0	−0.92	<500 K
		2.78×10^{12}	0	0	500−700 K
		4.42×10^{12}	0	0.92	>700 K
k_{-7}	$CHClCH_2OH \rightarrow C_2H_3Cl + OH$	2.52×10^{12}	0	30.94	<500 K
		9.74×10^{12}	0	30.94	500−700 K
		1.55×10^{13}	0	31.86	>700 K
k_8	$\dot{C}HClCH_2OH \rightarrow CH_2ClCH_2O^{\bullet}$	2.63×10^{7}	1.26	29.80	β
k_{-8}	$CH_2ClCH_2O^{\bullet} \rightarrow \dot{C}HClCH_2OH$	1.68×10^{8}	1.26	22.18	
k_9	$CH_2ClCH_2O^{\bullet} \rightarrow CH_2O + CH_2Cl$	3.52×10^{12}	0.042	18.51	
k_{10}	$CH_2ClCH_2O^{\bullet} \rightarrow CH_2ClCHO + H$	1.94×10^{9}	1.88	20.03	
k_{11}	$\dot{C}HClCH_2OH \rightarrow CHOH{=}CHCl + H$	3.10×10^{7}	1.69	37.65	

k_1	A_1 is taken half of (*E*)-CHCl=CHCl + OH;[28] E_{a1} is estimated to be 0 kcal/mol.
k_{-1}	from k_1, as well as the thermodynamics and microscopic reversibility ⟨*MR*⟩
k_2	A_2 from TST; E_{a2} = 6.2 kcal/mol[29]
k_{-2}	from k_2 and ⟨*MR*⟩
k_3	A_3 from TST; E_{a3} from E_{a-3}; E_{a-3} is estimated to be 0
k_4	A_4 from TST; E_{a4} from E_{a-4}; E_{a-4} is estimated to be 0
k_5	A_5 from TST; E_{a5} from E_{a-5}; E_{a-5} is calculated to be 3.56 kcal/mol (see text)
k_6	A_6 from TST; E_{a6} from $k(ClCH_2OH \rightarrow CH_2O + HCl)$[51] = 1.6×10^{-3} and we assume $A = 10^{13}$
k_7	from Villà et al.[4] and Yamada et al.[31]
k_{-7}	from k_7 and ⟨*MR*⟩
k_8	A_8 from TST; E_{a8} = 29.80 kcal/mol[31]
k_{-8}	from k_8 and ⟨*MR*⟩
k_9	A_9 from TST; E_{a9} from E_{a-9}; E_{a-9} = 7.3 from $C_2H_4 + CH_3$[47]
k_{10}	A_{10} from TST; E_{a10} from E_{a-10}; E_{a-10} = 2.4 from CH_3CHO + H[52]
k_{11}	A_{11} from TST; E_{a11} from E_{a-11}; E_{a-11} is calculated to be 4.56 kcal/mol (see text)

[a] A in $cm^3\ mol^{-1}\ s^{-1}$ or s^{-1}; E_a in kcal/mol. [b] Lennard-Jones parameters: σ = 4.55 Å; ϵ/k = 576.7 K.[32,33] [c] Reduced frequency sets (cm^{-1}) (from CPFIT[10]) are shown below:

	$CHClOH\dot{C}H_2$		$CH_2Cl\dot{C}HOH$		$\dot{C}HClCH_2OH$		$CH_2ClCH_2O^{\bullet}$	
vibration	freq	modes	freq	modes	freq	modes	freq	modes
1	375.1	6.383	396.7	6.046	250.5	4.652	519.0	6.761
2	1292.2	6.743	1180.6	6.515	1062.2	7.603	1380.4	7.207
3	3390.6	3.873	3051.1	4.439	3022.4	4.745	3234.8	3.532
mean	1011.7	17.000	1026.4	17.000	957.9	17.000	1123.4	17.500

High-pressure limit rate constants for input to the QRRK calculation are listed in Table 3. Preexponential *A* factors and E_a's for the bimolecular α- and β-addition reactions (k_1, k_7) are obtained from the evaluation of literature. The reverse reactions (k_{-1}, k_{-7}) are obtained by the analysis of thermodynamic properties of the relevant species and the application of microscopic reversibility ⟨*MR*⟩.

Unimolecular reactions of the adducts (k_2 to k_6, k_8 to k_{11}) are analyzed via TST and ⟨*MR*⟩ . Preexponential A factors for these unimolecular reactions are calculated with $A = (ekT/h)\exp(\Delta S^{\ddagger}/R)$. PM3 method in MOPAC6[16,17] is used to obtain the transition state structures and vibrational frequencies. The calculated transition state is identified by the presence of one negative frequency, analysis of geometry for that TS, and motion of the frequency. The imaginary frequency plus frequencies corresponding to low-energy intramolecular rotors are excluded from the MOPAC entropy and heat capacity calculations. Contributions to entropy and heat capacity from internal rotations using the method of Pitzer and Gwinn[18−21] are then incorporated. There are three methods to obtain the activation energies for these unimolecular reactions: (i) E_a for α-adduct isomerization (k_2), β-adduct isomerization (k_8), and HCl elimination from α-adduct (k_6) are from literature; (ii) E_a for Cl atom elimination reactions (k_3, k_4) and k_9 are calculated from the evaluation of literature E_a for the reverse addition/association reactions; (iii) k_5 and k_{11} are H atom elimination reactions with C=C bond formation. The barriers for these two reactions are obtained from the reverse addition reactions and ⟨*MR*⟩. We calculate E_a for H addition reactions to the C=C bonds by density functional methods at the B3LYP/6-31G(d,p) SCF = tight level in Gaussian 94. Frequencies are obtained at the same level and optimized geometry. The barrier for $CH_2{=}COHCl$ + H addition reaction ($E_{a(-5)}$) is calculated as 3.56 kcal/mol, it is higher than that for C_2H_4 + H which is between 2 and 3 kcal/mol.[27] Details on specific reaction rates are described below.

2a. α-Addition. The high-pressure limit rate constant for OH addition at the α-carbon of C_2H_3Cl (k_1) is obtained as follows: The Arrhenius preexponential factor is taken as one-half of literature value for (*E*)-CHCl=CHCl + OH[28] since the two carbon sites are identical in (*E*)-CHCl=CHCl. E_{a1} is estimated to be 0 kcal/mol because there is no observed barrier in experiments on OH addition to this double bond. This k_1 is slightly less than 10% of the overall addition ($k_1 + k_7$) and slightly higher than Kleindienst et al.[6]

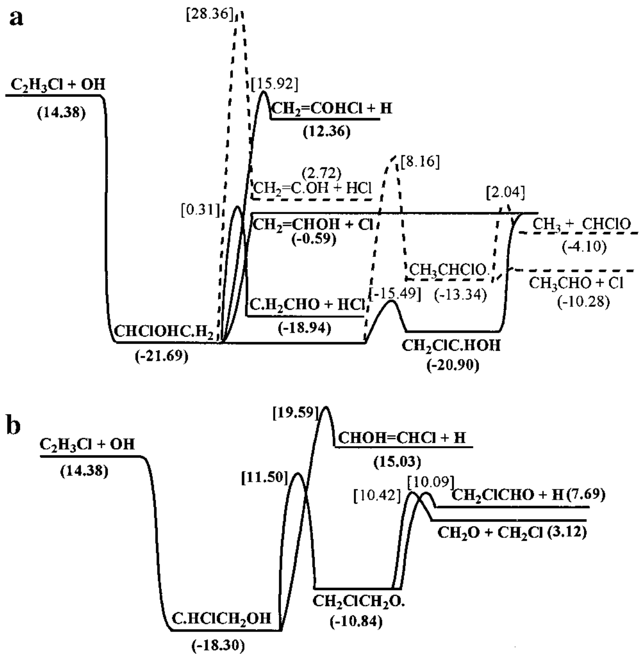

Figure 1. (a) Potential energy diagram of α-addition reaction system (kcal/mol). (b) Potential energy diagram of β-addition reaction system (kcal/mol).

OH addition to the α-carbon (k_1) forms the $CHClOH\dot{C}H_2^*$ energized adduct. This adduct has three dissociation channels: Cl elimination (k_4), HCl elimination reaction (k_6), and H elimination (k_5) which has a high ΔH_{rxn}, and therefore a much higher barrier, and is not important when this adduct is formed. This adduct can also undergo a 1,2-chlorine atom migration reaction (k_2). H elimination migration product, $CH_2Cl\dot{C}HOH$, has a low-energy dissociation channel: Cl elimination (k_3), which yields the same products as k_4.

It can be seen from Figure 1a that Cl migration, k_2, is the lowest energy channel for the α-addition adduct: $CHClOH\dot{C}H_2^* \rightarrow CH_2Cl\dot{C}HOH$; E_a for the Cl atom migration are calculated as 6.2 kcal/mol by Skell et al. using the multireference configuration interaction calculation method.[29] Perry et al. estimated this E_a as 3−5 kcal/mol.[2] Thermochemical estimation for this 1,2-Cl atom migration through a three-member cyclic transition state involving a third-row atom might be 12 to 19 kcal/mol.[8] The shift is not a critical step as the two important reactions are Cl atom elimination, both resulting in vinyl alcohol + Cl, and having similar energies. The subsequent Cl elimination reaction k_3, together with k_4, make vinyl alcohol + Cl atom the dominate products of this adduct's formation under most conditions (300−2000 K and 10^{-4}−10 atm). Other dissociations of this adduct (k_{-1}, k_5, and k_6) require higher energy than k_3 or k_4. E_a of the HCl elimination (k_6) is 22 kcal/mol (see Table 3), the Cl atom elimination reaction (k_3 or k_4) have lower barriers (19−19.8 kcal/mol), and these two reactions have similar preexponential A factors, so in this case the HCl elimination reaction has little effect on the overall rate constant. We note this HCl elimination may be important in a system where no lower energy path is present.

Several other possible reaction channels (shown in dashed lines in Figure 1a) are omitted due to their low contribution to the total rate constant. For example HCl elimination via a four-membered ring requires ca. 50 kcal/mol activation energy.[30] The barrier for hydroxyl H atom migration to the radical site via a four-membered ring is estimated to be 29.80 kcal/mol by ab initio calculations at CBS-q level.[31]

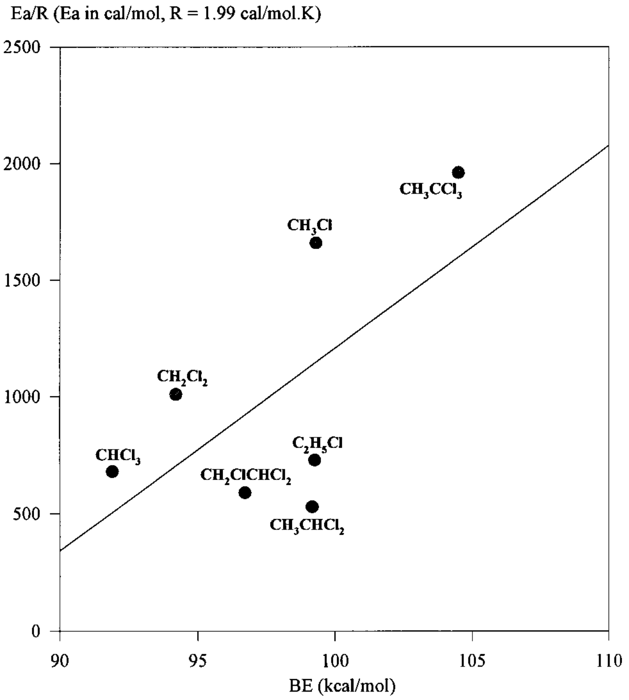

Figure 2. Modified Evans−Polanyi plot for OH abstraction of H atom from chlorinated hydrocarbons. Plot of E_a/R vs carbon−hydrogen bond energy. $E_a/R = 86.8(BE - 86.1)$.

2b. β-Addition. The rate constant for OH addition at the β-carbon (k_7) is referenced to the ab initio calculation on ethylene + OH addition reaction by Villà et al.[4] Their results showed that the rate constant parameters are strongly dependent on temperature. We take the preexponential A factor and $E_a(T)$ from Villà et al.[4] (see also Yamada et al.[31]). The reverse reaction (k_{-7}) is calculated from k_7 and $\langle MR \rangle$.

OH addition to the β-carbon of C_2H_3Cl (k_7) forms the $\dot{C}HClCH_2OH^*$ energized adduct. This adduct can undergo a hydroxyl H atom migration reaction k_8. A_8, n_8 are obtained from the TS in MOPAC6/PM3, E_{a8} = 29.80 kcal/mol is from the ab initio calculation.[31] There are three elimination/dissociation channels available for this β-adduct: k_9, k_{10}, and k_{11}. Unimolecular isomerization k_8 requires energy similar to that of the initial reactants. Relative small fractions of this adduct will isomerize (k_8) and further react even at higher temperature, due to the barrier and the tight transition state. The adduct is either stabilized or it dissociates back to the reactants (C_2H_3Cl + OH) via a loose transition state.

Lennard-Jones parameters in Table 3 are obtained from tabulations[32] and a calculation method based on molar volumes and compressibility.[33]

3. Transition-State-Theory Calculations for the Abstraction Reaction of C_2H_3Cl + OH. The α- and β-abstraction reactions are

$$C_2H_3Cl + OH \rightarrow CH_2{=}\dot{C}Cl + H_2O \qquad (a)$$

$$C_2H_3Cl + OH \rightarrow \dot{C}H{=}CHCl + H_2O \qquad (b)$$

3a. Estimation of E_a of Abstraction Reactions. A widely used method for estimating activation energy is offered by Evans and Polanyi:[34]

$$E_a = a\Delta H_{rxn} + b$$

where a and b are constants. ΔH_{rxn} is assumed to be proportional to the bond dissociation energy (BE) for a homologous reaction

TABLE 4: Summary of Contributions to $\Delta S^{\ddagger}$ for C_2H_3Cl + OH Abstraction Reaction [a,b]

type	ΔS_{trans}	ΔS_{vib}	ΔS_{rot}	ΔS_{ir}	ΔS_{el}	ΔS_{σ}	ΔS_n	$\Sigma\Delta S$	$\Delta S^{\ddagger}$
α-abs	0.72	1.30	3.48	9.05	1.38	0	0	15.93	−28.03
β-abs	0.72	1.30	3.20	9.05	1.38	0	0	15.65	−28.31

[a] All in cal/mol·K. [b] $\Delta S^{\ddagger} = S^{\ddagger} - S_{C_2H_3Cl} - S_{OH} = \Sigma\Delta S - S_{OH}$; see Table 1 for S_{OH}.

series; then

$$E_a/R = a'\text{BE} + b'$$

A modified Evans−Polanyi plot for OH abstraction of H atom from chlorinated hydrocarbons is illustrated in Figure 2. The E_a/R values are obtained from Cohen and Benson[35] with bond dissociation energies from the evaluation of the literature, which is described by Lay et al.[15] The regression result yields:

$$E_a/R = 86.8(\text{BE} - 86.1)$$

Here E_a in cal/mol, $R = 1.99$ cal/mol·K, so E_a/R is in units of K. BE is the C−H bond energy in kcal/mol.

The bond dissociation energies are evaluated to be 108.1 and 111.5 kcal/mol[15] for α- and β-abstraction of C_2H_3Cl + OH, respectively. From the above correlation we calculate the activation energies of 3.80 kcal/mol for α-abstraction and 4.39 kcal/mol for β-abstraction.

3b. Evaluation of Preexponential A Factors on Abstraction Reactions. The calculation of A factors for bimolecular abstraction reactions using transition-state-theory (TST) is described in detail by Cohen and co-workers.[34−37] For H atom transfer reactions, they suggest:

$$k(T) = 1.3 \times 10^{13} T^2 \exp(\Delta S^{\ddagger}/R)\exp(-E_a/RT) \times \text{reaction degeneracy}$$

The calculation for entropy of activation ($\Delta S^{\ddagger}$) requires knowledge of the activated complex, $C_2H_2Cl\cdots H\cdots OH$ (its bond lengths and angles, vibration frequencies, internal rotor parameters, electronic degeneracy, and symmetry properties) along with similar parameters of the reactants (C_2H_3Cl and OH).

$$\Delta S^{\ddagger} = S^{\ddagger} - S_{C_2H_3Cl} - S_{OH}, \quad \text{where } S^{\ddagger} \text{ is the entropy of TST complex}$$

We choose C_2H_3Cl as a model compound and then make corrections to the various degrees of freedom to obtain $S^{\ddagger}$:[35]

$$S^{\ddagger} = S_{C_2H_3Cl} + (\Delta S_{\text{trans}} + \Delta S_{\text{vib}} + \Delta S_{\text{rot}} + \Delta S_{\text{ir}} + \Delta S_{\text{el}} + \Delta S_{\sigma} + \Delta S_n) = S_{C_2H_3Cl} + \Sigma\Delta S$$

The calculation procedures are briefly described below, and the results are summarized in Table 4.

ΔS_{trans} depends only on the mass change between the TST complex and model compound, i.e., $\Delta S_{\text{trans}} = 1.5R \ln(M^{\ddagger}/M) = 0.72$ cal/mol·K.

We estimate the geometry of TST complex, then ΔS_{rot} is calculated knowing the product of moments of inertia of the complex and the reagent, $I^{\ddagger}$ and I, so:

$$\Delta S_{\text{rot,a}} = 0.5R \ln(I_a^{\ddagger}/I) = 3.48 \text{ cal/mol·K for α-abstraction}$$

$$\Delta S_{\text{rot,b}} = 0.5R \ln(I_b^{\ddagger}/I) = 3.20 \text{ cal/mol·K for β-abstraction}$$

The electronic degeneracy of the TST complex is 2 so that $\Delta S_{\text{el}} = R \ln 2$.

The external symmetry and the number of optical isomers of TST complex are unchanged from C_2H_3Cl, so $\Delta S_{\sigma} = R \ln(\sigma/\sigma^{\ddagger}) = 0$, and $\Delta S_n = R \ln(n^{\ddagger}/n) = 0$.

The contribution of the vibration frequencies ΔS_{vib} and internal rotations ΔS_{ir} to entropies and heat capacities of the activated complex are calculated by using a small computer code developed for this purpose. The frequency changes are obtained from tables of Benson[8] and Cohen.[35] Corrections to the entropy due to changes in the barrier to internal rotation are interpolated from tables developed by Pitzer and co-workers.[38] Cohen and Benson[35] analyzed the reactions of OH with haloalkanes and proposed that the entropy of free rotation about the C···H bond is 4.5 cal/mol·K and H···O bond is 4.3 for halomethanes. They reported values of 4.7 and 4.6 cal/mol·K for C···H and H···O bonds, respectively, in haloethanes. We take the average value of halomethanes and haloethanes for the C···H bond

$$\Delta S_{C\cdots H} = (4.5 + 4.7)/2 = 4.6$$

and the H···O bond

$$\Delta S_{H\cdots O} = (4.3 + 4.6)/2 = 4.45$$

Unlike the haloethanes, we do not have internal rotation about the C=C double bond. We assume:

$$\Delta S_{\text{ir}} = \Delta S_{C\cdots H} + \Delta S_{H\cdots O} = 4.6 + 4.45 = 9.05 \text{ cal/mol·K at 300 K}$$

The rate constants we obtain for the two abstraction channels (Table 4) are $k_a = 9.72 \times 10^6 T^2 \exp(-3800/RT)$ and $k_b = 1.69 \times 10^7 T^2 \exp(-4390/RT)$. The ratio of these two abstractions is $k_b/k_a = 1.74 \exp(-488/T)$.

A second method to estimate the Arrhenius A factors for specific H atom sites is to separate the observed experimental value for all H atoms into a sum where each term represents the contribution from specific H atom sites. Cohen suggested: "The probability of OH colliding with H is proportional to total cross section divided by number of available H atoms".[34] Incorporating this, the preexponential A factors for α- and β-abstraction from vinyl chloride are proportional to the number of available H atoms.

$$A_b/A_a = 2$$

This compares well with the ratio estimated from TST, 1.74.

Results and Discussion

The calculated rate parameters to all specific product sets are listed in Table 5.

Howard[1] has predicted that elimination of Cl from the adduct with formation of vinyl alcohol dominates for the α-addition due to the weaker C−Cl bond. Perry et al.[2] and Liu et al.[3] estimate the rate constant of this channel as a relatively minor reaction pathway of total rate constant. Our evaluation shows that OH addition to the α-carbon is a low fraction, ca. 10%, of that for addition to the β-carbon at room temperature under 1 atm; which is in agreement with the estimations of Perry et al.

TABLE 5: Overall Rate Constants $k = AT^n\exp(-E_a/RT)$ at Different Pressures[a,b]

reaction	A	n	E_a	remark
(a) 0.076 Torr				
$C_2H_3Cl + OH \rightarrow CH_2{=}\dot{C}Cl + H_2O$	9.72×10^{6}	2	3.80	α-abstraction
$C_2H_3Cl + OH \rightarrow \dot{C}H{=}CHCl + H_2O$	1.69×10^{7}	2	4.39	β-abstraction
$C_2H_3Cl + OH \rightarrow CHClOH\dot{C}H_2$	6.48×10^{-4}	−2.26	−1280	α-addition
$C_2H_3Cl + OH \rightarrow CH_2Cl\dot{C}HOH$	8.39×10^{-2}	−2.80	−213	
$C_2H_3Cl + OH \rightarrow CH_2{=}CHOH + Cl$	6.15×10^{11}	−0.12	103	
$C_2H_3Cl + OH \rightarrow CH_2{=}COHCl + H$	8.64×10^{-3}	3.72	1870	
$C_2H_3Cl + OH \rightarrow \dot{C}H_2CHO + HCl$	1.54×10^{9}	0.37	−171	
$C_2H_3Cl + OH \rightarrow \dot{C}HClCH_2OH$	6.12×10^{41}	−10.9	3550	β-addition
$C_2H_3Cl + OH \rightarrow CH_2ClCH_2O^{\bullet}$	9.33×10^{32}	−11.5	3510	
$C_2H_3Cl + OH \rightarrow CH_2O{+}CH_2Cl$	7.00×10^{9}	−0.46	−1930	
$C_2H_3Cl + OH \rightarrow CH_2ClCHO + H$	1.04×10^{5}	1.80	−2010	
$C_2H_3Cl + OH \rightarrow CHCl{=}CHOH + H$	5.98×10^{5}	1.93	5160	
$\dot{C}HClCH_2OH \rightarrow CH_2ClCH_2O^{\bullet}$	2.18×10^{-3}	3.14	22200	
$\dot{C}HClCH_2OH \rightarrow CHCl{=}CHOH + H$	6.75×10^{-84}	25.4	659	
(b) 0.76 Torr				
$C_2H_3Cl + OH \rightarrow CH_2{=}\dot{C}Cl + H_2O$	9.72×10^{6}	2	3.80	α-abstraction
$C_2H_3Cl + OH \rightarrow \dot{C}H{=}CHCl + H_2O$	1.69×10^{7}	2	4.39	β-abstraction
$C_2H_3Cl + OH \rightarrow CHClOH\dot{C}H_2$	9.46×10^{-11}	−0.09	−7500	α-addition
$C_2H_3Cl + OH \rightarrow CH_2Cl\dot{C}HOH$	1.79×10^{-8}	−0.67	−6260	
$C_2H_3Cl + OH \rightarrow CH_2{=}CHOH + Cl$	6.09×10^{11}	−0.12	100	
$C_2H_3Cl + OH \rightarrow CH_2{=}COHCl + H$	8.66×10^{-3}	3.72	1870	
$C_2H_3Cl + OH \rightarrow \dot{C}H_2CHO + HCl$	1.54×10^{9}	0.37	−171	
$C_2H_3Cl + OH \rightarrow \dot{C}HClCH_2OH$	2.67×10^{42}	−10.7	4740	β-addition
$C_2H_3Cl + OH \rightarrow CH_2ClCH_2O^{\bullet}$	4.87×10^{33}	−11.3	4150	
$C_2H_3Cl + OH \rightarrow CH_2O{+}CH_2Cl$	4.05×10^{12}	−1.25	−196	
$C_2H_3Cl + OH \rightarrow CH_2ClCHO + H$	5.48×10^{7}	1.02	−328	
$C_2H_3Cl + OH \rightarrow CHCl{=}CHOH + H$	6.18×10^{5}	1.93	5160	
$\dot{C}HClCH_2OH \rightarrow CH_2ClCH_2O^{\bullet}$	1.13×10^{32}	−7.40	34200	
$\dot{C}HClCH_2OH \rightarrow CHCl{=}CHOH + H$	1.73×10^{19}	−5.48	32900	
(c) 7.6 Torr				
$C_2H_3Cl + OH \rightarrow CH_2{=}\dot{C}Cl + H_2O$	9.72×10^{6}	2	3.80	α-abstraction
$C_2H_3Cl + OH \rightarrow \dot{C}H{=}CHCl + H_2O$	1.69×10^{7}	2	4.39	β-abstraction
$C_2H_3Cl + OH \rightarrow CHClOH\dot{C}H_2$	5.04×10^{6}	−5.05	−8850	α-addition
$C_2H_3Cl + OH \rightarrow CH_2Cl\dot{C}HOH$	4.50×10^{3}	−4.07	−9670	
$C_2H_3Cl + OH \rightarrow CH_2{=}CHOH + Cl$	6.09×10^{11}	−0.12	100	
$C_2H_3Cl + OH \rightarrow CH_2{=}COHCl + H$	8.83×10^{-3}	3.72	1880	
$C_2H_3Cl + OH \rightarrow \dot{C}H_2CHO + HCl$	1.55×10^{9}	0.37	−170	
$C_2H_3Cl + OH \rightarrow \dot{C}HClCH_2OH$	3.63×10^{43}	−10.7	6210	β-addition
$C_2H_3Cl + OH \rightarrow CH_2ClCH_2O^{\bullet}$	5.04×10^{35}	−11.4	4710	
$C_2H_3Cl + OH \rightarrow CH_2O{+}CH_2Cl$	1.78×10^{16}	−2.28	2270	
$C_2H_3Cl + OH \rightarrow CH_2ClCHO + H$	2.82×10^{11}	−0.03	2140	
$C_2H_3Cl + OH \rightarrow CHCl{=}CHOH + H$	4.19×10^{6}	1.69	5640	
$\dot{C}HClCH_2OH \rightarrow CH_2ClCH_2O^{\bullet}$	4.20×10^{32}	−7.32	35200	
$\dot{C}HClCH_2OH \rightarrow CHCl{=}CHOH + H$	1.97×10^{31}	−8.00	38300	
(d) 76 Torr				
$C_2H_3Cl + OH \rightarrow CH_2{=}\dot{C}Cl + H_2O$	9.72×10^{6}	2	3.80	α-abstraction
$C_2H_3Cl + OH \rightarrow \dot{C}H{=}CHCl + H_2O$	1.69×10^{7}	2	4.39	β-abstraction
$C_2H_3Cl + OH \rightarrow CHClOH\dot{C}H_2$	1.80×10^{68}	−22.7	7500	α-addition
$C_2H_3Cl + OH \rightarrow CH_2Cl\dot{C}HOH$	3.95×10^{66}	−22.2	6900	
$C_2H_3Cl + OH \rightarrow CH_2{=}CHOH + Cl$	6.09×10^{11}	−0.12	100	
$C_2H_3Cl + OH \rightarrow CH_2{=}COHCl + H$	1.08×10^{-2}	3.69	1930	
$C_2H_3Cl + OH \rightarrow \dot{C}H_2CHO + HCl$	1.59×10^{9}	0.37	−162	
$C_2H_3Cl + OH \rightarrow \dot{C}HClCH_2OH$	1.48×10^{43}	−10.3	7190	β-addition
$C_2H_3Cl + OH \rightarrow CH_2ClCH_2O^{\bullet}$	3.17×10^{35}	−10.9	4200	
$C_2H_3Cl + OH \rightarrow CH_2O{+}CH_2Cl$	2.25×10^{19}	−3.13	4880	
$C_2H_3Cl + OH \rightarrow CH_2ClCHO + H$	6.40×10^{14}	−0.96	4830	
$C_2H_3Cl + OH \rightarrow CHCl{=}CHOH + H$	2.03×10^{10}	0.63	7830	
$\dot{C}HClCH_2OH \rightarrow CH_2ClCH_2O^{\bullet}$	1.64×10^{34}	−7.58	36500	
$\dot{C}HClCH_2OH \rightarrow CHCl{=}CHOH + H$	5.85×10^{39}	−9.70	43400	
(e) 760 Torr				
$C_2H_3Cl + OH \rightarrow CH_2{=}\dot{C}Cl + H_2O$	9.72×10^{6}	2	3.80	α-abstraction
$C_2H_3Cl + OH \rightarrow \dot{C}H{=}CHCl + H_2O$	1.69×10^{7}	2	4.39	β-abstraction
$C_2H_3Cl + OH \rightarrow CHClOH\dot{C}H_2$	1.22×10^{84}	−25.5	15000	α-addition
$C_2H_3Cl + OH \rightarrow CH_2Cl\dot{C}HOH$	1.27×10^{84}	−25.5	14900	

TABLE 5: (Continued)

reaction	A	n	E_a	remark
(e) 760 Torr (Continued)				
$C_2H_3Cl + OH \rightarrow CH_2{=}CHOH + Cl$	1.22×10^{12}	−0.20	274	
$C_2H_3Cl + OH \rightarrow CH_2{=}COHCl + H$	5.70×10^{-2}	3.49	2380	
$C_2H_3Cl + OH \rightarrow \dot{C}H_2CHO + HCl$	4.13×10^{9}	0.25	87	
$C_2H_3Cl + OH \rightarrow \dot{C}HClCH_2OH$	1.77×10^{40}	−9.08	7240	β-addition
$C_2H_3Cl + OH \rightarrow CH_2ClCH_2O^{\bullet}$	1.11×10^{43}	−12.7	7150	
$C_2H_3Cl + OH \rightarrow CH_2O{+}CH_2Cl$	7.76×10^{19}	−3.22	6740	
$C_2H_3Cl + OH \rightarrow CH_2ClCHO + H$	5.89×10^{15}	−1.17	6850	
$C_2H_3Cl + OH \rightarrow CHCl{=}CHOH + H$	2.54×10^{14}	−0.52	10800	
$\dot{C}HClCH_2OH \rightarrow CH_2ClCH_2O^{\bullet}$	2.12×10^{31}	−6.48	36300	
$\dot{C}HClCH_2OH \rightarrow CHCl{=}CHOH + H$	1.01×10^{40}	−9.16	45400	
(f) 7600 Torr				
$C_2H_3Cl + OH \rightarrow CH_2{=}\dot{C}Cl + H_2O$	9.72×10^{6}	2	3.80	α-abstraction
$C_2H_3Cl + OH \rightarrow \dot{C}H{=}CHCl + H_2O$	1.69×10^{7}	2	4.39	β-abstraction
$C_2H_3Cl + OH \rightarrow CHClOH\dot{C}H_2$	1.25×10^{83}	−23.7	18500	α-addition
$C_2H_3Cl + OH \rightarrow CH_2Cl\dot{C}HOH$	1.22×10^{83}	−23.7	18300	
$C_2H_3Cl + OH \rightarrow CH_2{=}CHOH + Cl$	6.75×10^{14}	−0.98	2090	
$C_2H_3Cl + OH \rightarrow CH_2{=}COHCl + H$	14.0	2.81	4050	
$C_2H_3Cl + OH \rightarrow \dot{C}H_2CHO + HCl$	1.78×10^{12}	−0.50	1880	
$C_2H_3Cl + OH \rightarrow \dot{C}HClCH_2OH$	3.56×10^{34}	−7.11	6190	β-addition
$C_2H_3Cl + OH \rightarrow CH_2ClCH_2O^{\bullet}$	1.05×10^{46}	−12.9	10400	
$C_2H_3Cl + OH \rightarrow CH_2O{+}CH_2Cl$	3.86×10^{17}	−2.46	7820	
$C_2H_3Cl + OH \rightarrow CH_2ClCHO + H$	6.64×10^{13}	−0.52	8080	
$C_2H_3Cl + OH \rightarrow CHCl{=}CHOH + H$	3.92×10^{14}	−0.50	12500	
$\dot{C}HClCH_2OH \rightarrow CH_2ClCH_2O^{\bullet}$	1.35×10^{26}	−4.71	35300	
$\dot{C}HClCH_2OH \rightarrow CHCl{=}CHOH + H$	4.04×10^{34}	−7.08	45100	

[a] k and A in $cm^3\ mol^{-1}\ s^{-1}$ or s^{-1}; T in K; E_a in cal/mol; and n is unitless. [b] 300−2000 K.

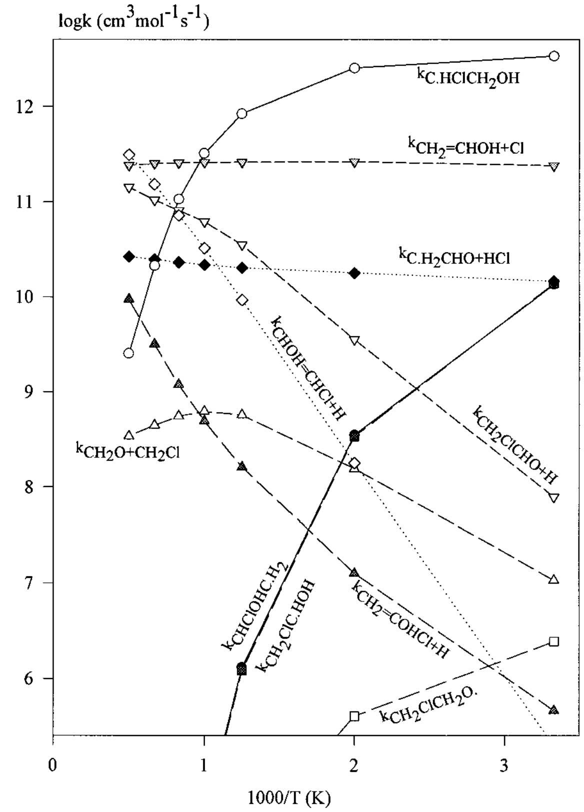

Figure 3. Addition rate constants vs temperature at 1 atm.

and Liu et al. Formation of the β-adduct (stabilized) is the dominant addition product at 1 atm and 298−1000 K.

Figure 3 shows the calculated rate constants versus temperature for both α- and β-addition paths at 1 atm. Addition at the β-carbon and $\dot{C}HClCH_2OH$ adduct stabilization is the most important channel below 1000 K at 1 atm. α-Addition is about 100 times slower than β-addition between 300−2000 K. The β-stabilization rate constant decreases with increasing temperature (falloff), while the α reaction which goes to the low-energy vinyl alcohol + Cl product remains near constant. Reverse reaction of the β adduct, dissociation to vinyl chloride + OH, increases with temperature and dominates stabilization above ca. 800 K (experimentally observed as reduced reaction rate or negative activation energy), as previously reported by Liu et al.[3]

The α-adduct channel behaves differently than β-addition due to the low-energy reaction channels available to this adduct—most of the α-adduct rapidly undergoes Cl elimination, or Cl shift, and then elimination of Cl, both paths resulting in vinyl alcohol + Cl atom products. We calculate that the vinyl alcohol + Cl atom products dominate for the α-addition channel at 300 to 2000 K and 10^{-4} to 10 atm. The energy barrier for Cl elimination from the α-adduct is 19.88 kcal/mol relative to the stabilized adduct, with the estimated preexponential factor of $9.36 \times 10^{11}\ s^{-1}$ (see Table 3); this provides a half-life of ca. 90 s at 298 K. This half-life is sufficient that the α-adduct, if stabilized, will react with O_2 under atmospheric conditions to form a chloro-hydroxyl peroxy radical. When temperature increases to 950 K, the half-life of this Cl elimination decreases to ca. 10^{-8} second so that dissociation occurs before reaction with O_2 under combustion conditions. The vinyl alcohol + Cl channel dominates all other product reactions from α-addition, and all new products resulting from β-addition in the temperature range 300−1500 K (excluding β-adduct stabilization). A small fraction, near constant 10%, of the overall reaction proceeds to vinyl alcohol + Cl product below 1000 K due to the α-addition rate constant. This fraction of the overall rate constant is in agreement with previous studies.[2,3] As temperature increases, other product channels start to show importance. CHOH=CHCl + H is an important product channel above 1500 K which results from β-adduct elimination of H atom.

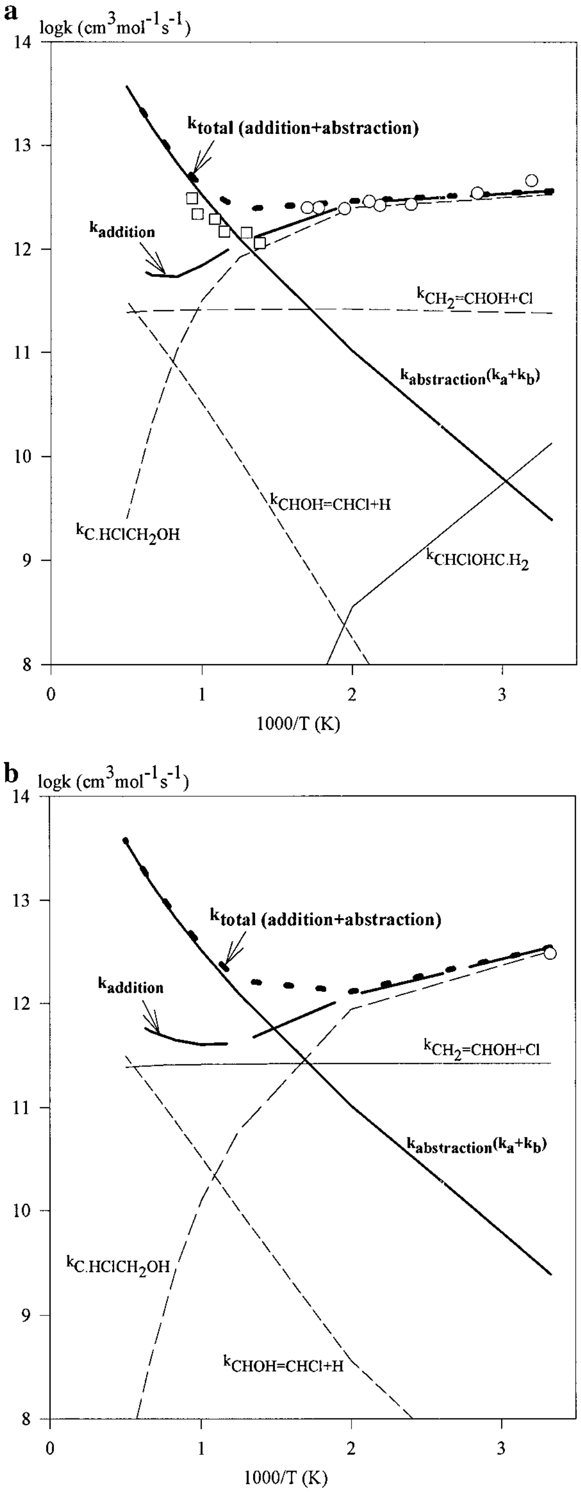

Figure 4. (a) Comparison of model with experiment (Liu et al.[3]): temperature-dependent rate constants at 1 atm: (○) addition; (□) abstraction. (b) Comparison of model with experiment (Howard[1]): temperature-dependent rate constants at 10^{-2} atm (○) at 7 Torr.

Figure 4a compares calculated rate constants of the important addition channels with the experiments over the temperature range 300−2000 K at 760 Torr. The sum of abstraction rate constants ($k_a + k_b$) calculated by transition-state-theory are also shown in Figure 4a. The abstraction reactions starts to dominate over addition from 810 K, while Liu et al.[3] reported that it dominates above 723 K. The overall rate constant—addition plus abstraction—is shown to be in agreement with the experimental data.

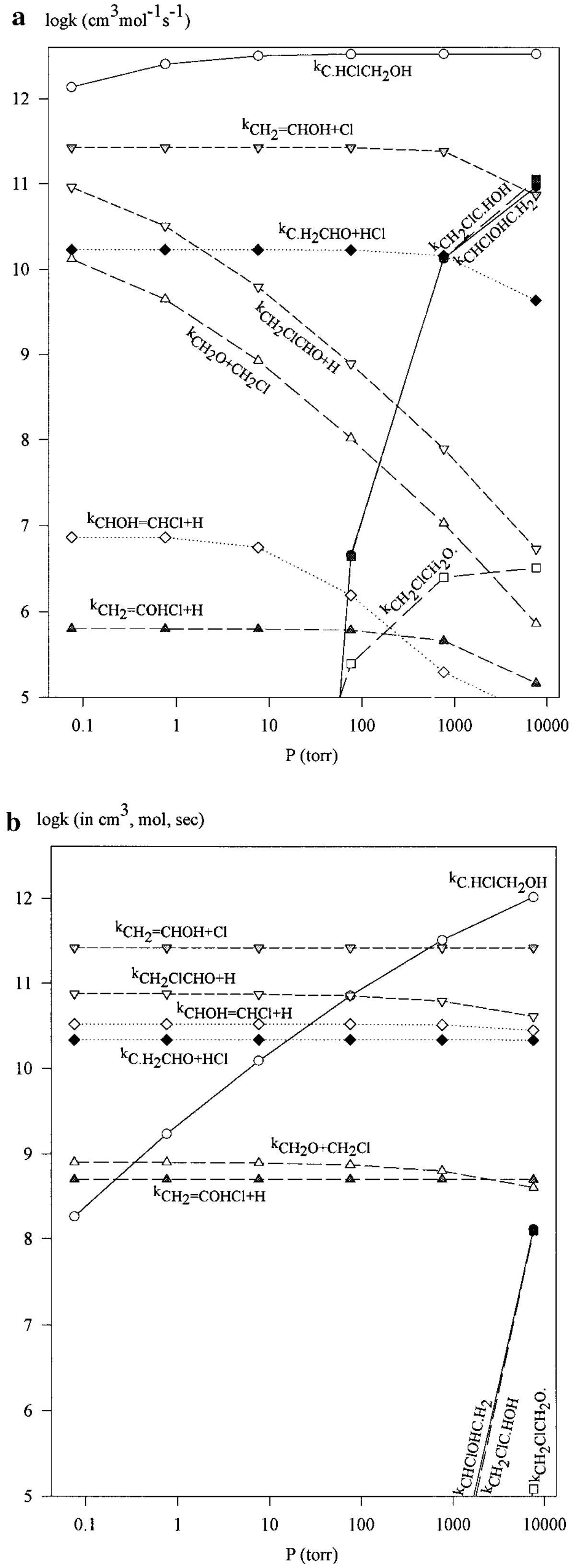

Figure 5. (a) Addition rate constants vs pressure at 300 K. (b) Addition rate constants vs pressure at 1000 K.

Figure 4b compares calculated rate constants vs temperature at 0.01 atm and again shows good agreement with the experimental data. Vinyl alcohol + Cl is the most important addition product channel at low and moderate temperature, while

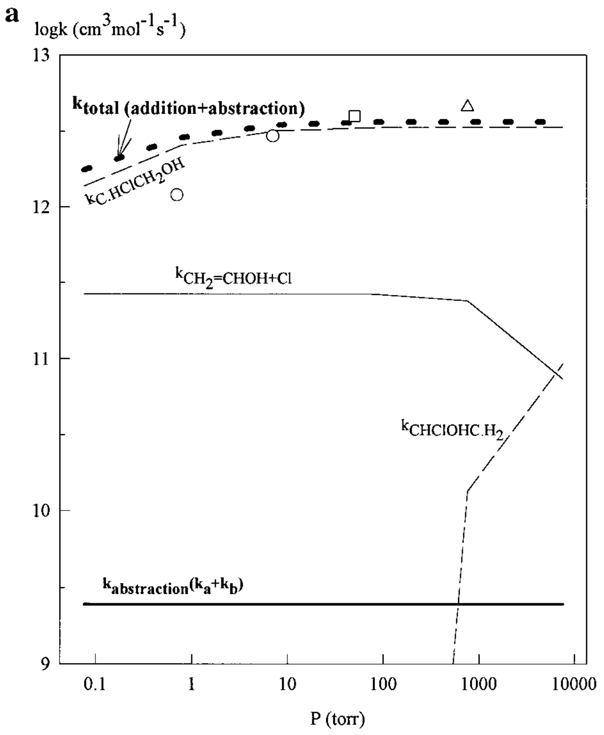

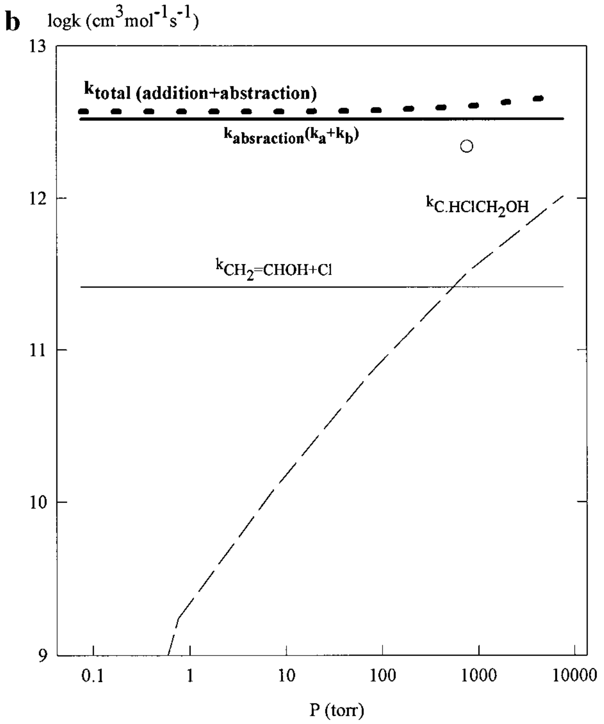

Figure 6. (a) Comparison of model with experiment: pressure dependent rate constants at 300 K (○ Howard;[1] □ Perry et al.;[2] △ Liu et al.[3]). (b) Comparison of model with experiment (Liu et al.[3]): pressure dependent rate constants at 1000 K (○) at 1033 K.

$CHOH{=}CHCl + H$ starts to dominant when temperature approaches 2000 K.

The rate constants versus pressure at 300 K for the addition reaction channels are illustrated in Figure 5a. The β-addition channel is dominate at high pressure and in the falloff regime as suggested by previous researchers.[1-3] Figure 5b illustrates this rate constant versus pressure at 1000 K. The rate constant for β-adduct formation, $\dot{C}HClCH_2OH$ undergoes rapid falloff with decreasing pressure. Vinyl alcohol + Cl and $CHOH{=}CHCl + H$ from H elimination of the β-adduct are the dominant products below 760 Torr.

The comparison of calculated rate constants with experimental data[1-3] at 300 K versus pressure is shown in Figure 6a. The experimental data (0.7 to 7 Torr) of Howard[1] was extrapolated using a curved Lindemann plot[2] and estimated as $k_{\mathrm{inf}} \approx 4.20 \times 10^{12}$ cm^3 mol^{-1} s^{-1} at 100 Torr for the reaction of OH with C_2H_3Cl. Perry et al.[2] observed no pressure dependence and proposed that their work at 50 Torr were at the high-pressure limit and estimated a value of $k \approx 3.97 \times 10^{12}$ cm^3 mol^{-1} s^{-1}. Liu et al.[3] measured this rate constant to be 4.55×10^{12} cm^3 mol^{-1} s^{-1} at 760 Torr. The model shows the same pressure dependence as these research groups. We predict the reaction is at 95% of high-pressure limit by 7 Torr with a small, ca. 5% increase, between 7 and 760 Torr as illustrated in Figure 6a.

The calculated important rate constants at 1000 K versus pressure are plotted in Figure 6b. Experimental data by Liu et al.[3] at 1033 K are also shown. Abstractions ($k_a + k_b$) are the dominate reaction channels, when the temperature increases to 1000 K.

Data in Figures 3−6 illustrate that the β-addition adduct is one of the most important species at 300−1000 K and 10^{-4}−10 atm; so it is of value to study its fate under different conditions. Under atmospheric conditions this β-adduct $\dot{C}HClCH_2$-OH is stable and will react with O_2 and then nitric oxide to form a chloro-alkoxy radical ($CH_2OHCHClO^{\bullet}$). This chloro-alkoxy radical has two low-energy channels for unimolecular dissociation, both involving carbonyl formation: (i) HCl elimination to $HCl + CH_2OH\dot{C}{=}O$, and (ii) Cl atom elimination to $Cl + CH_2OHCHO$. Kaiser and Wallington indicate HCl elimination is dominant in the methyl analogue.[39,40]

The enthalpies of important species are critical to our kinetic calculation (see Table 1). The kinetic estimates on several reaction paths are, therefore, dependent on correct product and/or reactant enthalpies. $\Delta H_f°_{298}$ of C_2H_3Cl is evaluated to be 5.06 kcal/mol, which differs from literature data: 6.81[41] or 8.40,[42] but our value is in good agreement with Melius's BAC-MP4 result (4.7)[43] and Colegrove's G2 calculation (5.00).[44] Colegrove also suggested that the reported experimental values of $\Delta H_f°_{298}(C_2H_3Cl)$[41,42] need to be reexamined. Vinyl alcohol is calculated as −29.95 and −29.46 kcal/mol by CBS-APNO and G2 methods, respectively.[31] Turecek et al.[45] reported the $\Delta H_f°_{298}$ of vinyl alcohol as −29.6 kcal/mol using G2MP2. Smith et al.[46] calculated energy of vinyl alcohol relative to acetaldehyde using G1; their calculation result is 11.23 kcal/mol above acetaldehyde, which places $\Delta H_f°_{298}$ of vinyl alcohol at −28.53 kcal/mol. Our evaluation (−29.61 kcal/mol) is consistent with above values. The errors in $\Delta H_f°_{298}$ of vinyl alcohol and $\dot{C}H_2CHOH$ radical are estimated to be less than ±1.5 kcal/mol.[11,12] The barrier height of H atom migration reaction (E_{a8}) from CBS-q calculation is estimated having −2 to +1 kcal/mol error bar.[31] This error does not have much effect on the rate constants of dissociation products: $CH_2ClCHO + H$ and $CH_2O + CH_2Cl$ because E_a is predominantly controlled by ΔH_{rxn}. The uncertainty for H atom addition to a carbon−carbon double bond (such as $E_{a(-5)}$ and $E_{a(-11)}$ in this work) is estimated as ±1 kcal/mol. E_a's for H addition in the literature[47] range from up to 3 kcal/mol for ethylene to 0 kcal/mol for isobutene. Barriers and reaction enthalpies are noted in the text and in the listed reaction kinetic parameters for input to QRRK calculations.

Summary

The reaction system of vinyl chloride with OH radical is complex: It involves four initial reaction pathways: α- and

β-addition and α- and β-abstraction plus nine isomerization or dissociation channels of the adducts formed via the additions. The two abstraction paths are analyzed using a modified Evans–Polanyi relation for activation energy and transition-state-theory for Arrhenius A factors. Addition reactions are analyzed using chemical activation formalism based on a multifrequency QRRK calculation for $k(E)$ and master equation analysis for falloff. Rate constants and reaction paths are predicted versus temperature and pressure and compared with experimental data. The calculations serve as useful estimates for rate constants and reaction paths in applications of combustion and atmospheric modeling (pressure and temperature) regimes, where experimental data are not available.

Acknowledgment. The authors gratefully acknowledge funding from the USEPA Northeast Research Center and the USEPA-CalTech-MIT-NJIT Research Center on Airborne Organics. We also acknowledge Jeff Ing, Albert Y. Chang, and Chad Sheng for help with the master equation code.

References and Notes

(1) Howard, C. J. *J. Chem. Phys.* **1976**, *65*, 4771.

(2) Perry, R. A.; Atkinson, R.; Pitts, J. N., Jr. *J. Chem. Phys*. **1977**, *67*, 458.

(3) Liu, A.; Mulac, W. A.; Jonah, C. D. *J. Phys. Chem.* **1989**, *93*, 4092.

(4) Villà, J.; González-Lafont, A.; Lluch, J. M.; Corchado, J. C.; Espinosa-García, J. *J. Chem. Phys.* **1997**, *107*, 7266.

(5) Sekušak, S.; Liedl, K. R.; Sabljic, A. *J. Phys. Chem.* **1998**, *102*, 1583.

(6) Kleindienst, T. E.; Shepson, P. B.; Nero, C. M.; Bufalini, J. J. *Int. J. Chem. kinetics* **1989**, *21*, 863.

(7) (a) Gilbert, R. G.; Smith, S. C. *Theory of Unimolecular and Recombination Reactions*; Oxford Press: New York, 1990. (b) Gilbert, R. G.; Smith, S. C.; Jordan, M. J. T. *UNIMOL Program Suite (Calulation of Falloff Curve for Unimolecular and Recombination Reactions)*, 1993. Available from the authors: School of Chemistry, Sidney University, NSW 2006, Australia, or by email to gilbert_r@summer.chem.su.oz.au. (c) Dean, A. M.; Chang, A. Y. Personal Communication. Exxon Corp. Res., Annandale, NJ. (d) Gilbert, R. G.; Luther, K.; Troe, J. *Ber. Bunsen-Ges. Phys. Chem.* **1983**, *87*, 169.

(8) Benson, S. W. *Thermochemical Kinetics*; John Wiley: New York, 1976.

(9) Ritter, E. R.; Bozzelli, J. W. *Int. J. Chem. Kinet.* **1991**, *23*, 767.

(10) Ritter, E. R. *J. Chem. Info. Comput. Sci.* **1991**, *31*, 400.

(11) Chen, Chiung-ju; Wong, D.; Bozzelli, J. W. *J. Phys. Chem*. **1998**, *102*, 4551.

(12) Zhu, L.; Bozzelli, J. W.; Lay, T. H. *Ind. Eng. Chem. Res.* **1998**, *37*, 3497.

(13) Lay, T. H.; Bozzelli, J. W. *J. Phys. Chem*. **1997**, *101*, 9505.

(14) Chen, Y.; Tschuikow-Roux, E. *J. Phys. Chem*. **1992**, *96*, 7266.

(15) Lay, T. H.; Bozzelli, J. W.; Dean, A. M.; Ritter, E. R. *J. Phys. Chem*. **1995**, *99*, 14514.

(16) *MOPAC: A General Molecular Orbital Package* (QCPE 455): *QCPE Bull.* **1983**, *3*, 43.

(17) Stewart, J. J. P. *MOPAC6.0*, Frank J. Seiler Research Lab., US Air Force Academy: CO, 1990.

(18) Pitzer, K. S. *J. Chem. Phys.* **1937**, *5*, 469.

(19) Pitzer, K. S. *J. Chem. Phys*. **1946**, *14*, 239.

(20) Pitzer, K. S.; Gwinn, W. D. *J. Chem. Phys.* **1942**, *10*, 428.

(21) Kilpatrick, J. E.; Pitzer, K. S. *J. Chem. Phys*. **1949**, *11*, 1064.

(22) Yamada, T.; Bozzelli, J. W.; Lay, T. *Twenty Seventh Symp. (Int.) Combust. [Proc.]* **1998**, 201.

(23) Stull, D. R.; Prophet, H. *JANAF Thermochemical Tables*, 2nd ed.; *(NSRDS-NBS 37)*; U.S. Government Printing Office: Washington D.C., 1971.

(24) Frenkel, M.; Kabo, G. J.; Marsh, K. N.; Roganov, G. N.; Wilhoit, R. C. *Thermodynamics of Organic Compounds in the Gas State*; Texas A&M Research Center: College Station, TX, 1994.

(25) Chang, A. Y.; Bozzelli, J. W.; Dean, A. M., submitted for publication.

(26) Bozzelli, J. W.; Chang, A. Y.; Dean, A. M. *Int. J. Chem. Kinet.* **1997**, *29*, 161.

(27) Lightfoot, P. D.; Pilling, M. J. *J. Phys. Chem.* **1987**, *91*, 3373.

(28) Zhang, Z.; Liu, R.; Huie, R. E.; Kurylo, M. J. *J. Phys. Chem*. **1991**, *95*, 194.

(29) Engels, B.; Peyerimhoff, S. D.; Skell, P. S. *J. Phys. Chem*. **1990**, *94*, 1267.

(30) Hassler, J. C.; Setser, D. W. *J. Chem. Phys.* **1966**, *45*, 3246.

(31) Yamada, T.; Bozzelli, J. W. Kinetic and Thermodynamic Analysis on OH Addition to Ethylene: Adduct Stabilization, Isomerization, and Isomer Dissociation. *J. Phys. Chem. A* **1999**, *103*, 7646.

(32) Reid, R. C.; Prausnitz, J. M.; Polling, B. E. *Properties of Gases and Liquids*, 4th ed.; McGraw-Hill: New York, 1989.

(33) Ben-Amotz, D.; Herschbach, D. R. *J. Phys. Chem.* **1990**, *94*, 1038.

(34) Cohen, N. *Int. J. Chem. Kinet.* **1982**, *14*, 1339.

(35) Cohen, N.; Benson, S. W. *J. Phys. Chem.* **1987**, *91*, 162.

(36) Cohen, N.; Westberg, K. R. *Int. J. Chem. Kinet.* **1986**, *18*, 99.

(37) Cohen, N. *Int. J. Chem. Kinet.* **1989**, *21*, 909.

(38) Lewis, G. N.; Randall, M.; Pitzer, K. S.; Brewer, L. *Thermodynamics*, 2nd ed.; McGraw-Hill: New York, 1961.

(39) Maricq, M. M.; Shi, J.; Szente, J. J.; Kaiser, E. W. *J. Phys. Chem.* **1993**, *97*, 9586.

(40) Kaiser, E. W.; Wallington, T. J. *J. Phys. Chem.* **1995**, *99*, 8669.

(41) Rodgers, A. S. *Selected Values for Properties of Chemical Compounds*; Thermodynamic Research Center, Texas A&M University: College Station, TX, 1982.

(42) Stull, D. R.; Westrum, E. F., Jr.; Sinke, G. C. *The Chemical Thermodynamics of Organic Compounds*; Robert E. Krieger Publishing: Malabar, FL, 1987; Chapter 14.

(43) Melius, C. F. *BAC-MP4 Heats of Formation and Free Energies*; Sandia National Laboratories: Livermore, CA, 1993.

(44) Colegrove, B. T.; Thompson, T. B. *J. Chem. Phys.* **1997**, *106*, 1480.

(45) Turecek, F.; Cramer, C. J. *J. Am. Chem. Soc.* **1995**, *117*, 12243.

(46) Smith, I. W. M.; Zellner, R. *J. Chem. Soc., Faraday Trans. 2* **1973**, *69*, 1617.

(47) Kerr, J. A.; Parsonage, M. J. *Evaluated Kinetic Data on Gas-Phase Addition Reactions: Reactions of Atoms and Radicals with Alkenes, Alkynes and Aromatic Compounds*; Butterworth: London, 1972.

(48) Tschuikow-Roux, E.; Paddison, S. *Int. J. Chem. Kinet.* **1987**, *19*, 16.

(49) Taylor, P. H.; Dellinger, B.; Tirey, D. A. *Int. J. Chem. Kinet.* **1991**, *23*, 1051.

(50) Scott, A. P.; Radom, L. *J. Phys. Chem.* **1996**, *100*, 16502.

(51) Tyndall, G. S.; Wallington, T. J.; Hurley, M. D.; Schneider, W. F. *J. Phys. Chem*. **1993**, *97*, 1576.

(52) Baulch, D. L.; Cobos, C. J.; Cox, R. A.; Esser, C.; Frank, P.; Just, T.; Kerr, J. A.; Pilling, M. J.; Troe, J.; Walker, R. W.; Warnatz, J. *J. Phys. Chem. Ref. Data* **1992**, *21*, 411.